INVERSE DYNAMICS CONTROL FOR A 3DOF QUADROTOR

Mauricio Becerra-Vargas, maubeus@sc.usp.br
Eduardo Morgado Belo, belo@sc.usp.br
Engineering School of Sao Carlos - University of Sao Paulo, 13566-590 Sao Carlos - SP, Brazil

Abstract. *The purpose of this study is to apply inverse dynamics control for attitude control of a quadrotor. A nonlinear model of an six degrees of freedom (6 DOF) quadrotor UAV is derived. Imperfect compensation of the inverse dynamic control is intentionally introduced in order to simplify the implementation of this approach and external disturbances are considered. The control strategy is applied in the outer loop of the inverse dynamic control to counteract the effects of imperfect compensation and external disturbances. The control strategy is designed using Lyapunov stability theory (LST).*

Keywords: Quadrotor UAV, Inverse Dynamics Control, Lyapunov stability, Robust Control

1. INTRODUCTION

A quadrotor UAV is a unmanned aerial vehicels whose lift is generated by four rotors, and it has gained a lot of attention since the first military applications.

In most motion control schemes concerning quadrotor UAVs the efects of the quadrotor dynamics are ignored or a linearized model is used as is shown in Bouabdallah *et al.* (2004), Bauer *et al.* (2008) and Goel *et al.* (2009). Nonlinear control schemes based on inverse dynamic control as sliding mode control and backstepping control are used to robustify the control system against model errors, parametric uncertainties and other disturbances as is shown in Xu and Ozguner (2006), Bouabdallah and Siegwart (2007), Benallegue *et al.* (2008), Mian and Daobo (2008), Lee *et al.* (2009) and Guisser and Medromi (2009). In Mokhtari *et al.* (2007), a mixed inverse dynamic control with a linear H_∞ controller and a sliding mode observer is applied to a non linear quadrotor UAV.

Inverse dynamics control is an approach to nonlinear control design of which the central idea is to construct an inner loop control based on the motion base dynamic model which, in the ideal case, exactly linearizes the nonlinear system and an outer loop control to drive tracking errors to zero. Nonetheless, this technique is based on the assumption of exact cancellation of nonlinear terms, therefore, parametric uncertainty, unmodeled dynamics and external disturbances may deteriorate the controller performance. Robustness can be regained by applying robust control tecniques in the outer loop control structure as is shown in Becerra-Vargas *et al.* (2009) .

In this context, this work presents the application of a inverse dynamic control, usually applied to control of robotics manipulators, to a attitude control of a 3DOF quadrotor manipulator. The dynamic model of 6DOF quadrotor is developed. The control strategy consist of the introducing an additional term to the inverse dynamics controller which provides robustness to the control system. The robust control term is designed by providing stability, through Laypunov stability theory (LST), of the linearized state system in the presence of uncertainties. This control term presents a phenomenon known as chattering. Therefore, a saturation function is adopted to replace the control law. Finally, a pitch trajectory is used to evaluate the performance of the controller.

2. QUADROTOR MODELLING

The quadrotor configuration consists mainly of four electrically driven fixed-pitch propellers equally spaced in a shape of a cross as is shown in Fig. 1. One sets of propellers rotates clockwise (Motors 2 and 4), the other counterclockwise (Motors 1 and 3). In that spin configuration, the equilibrium is achieved by providing all of the propellers spin at the same speed, resulting in zero torque about the body axes and uniform thust. Angular and linear motion are obtained by increasing and reducing the speed of the motors.

The dynamic model is derived under the following assumptions: the structure is supposed to be rigid; the structure is supposed symmetrical; the center of mass and the body fixed frame origin are assumed to coincide; the propellers are supposed rigid and the thrust and drag are proportional to the square of the propeller speed.

2.1 Translation and rotational dynamic model

In this paper, leading superscripts identify which coordinate system a vector is written in. For example, $\mathbf{F}^E$ represents a force vector written in frame {**E**}.

To perform the dynamic modelling of the quadrotor, we define the inertial frame {**E**} (North-East-Down orientation) and the body frame {**B**} fixed with the quadrotor as shown in Fig. 2. The orientation of the frame {**B**} respect to the frame {**E**} is given by three consecutive rotation (yaw-pitch-roll Euler angles), where each rotation takes place about an axis whose location depends upon the preceding rotations (Fig. 2). The rotation matrix $\mathfrak{R}$ is obtained by post-multiplying the
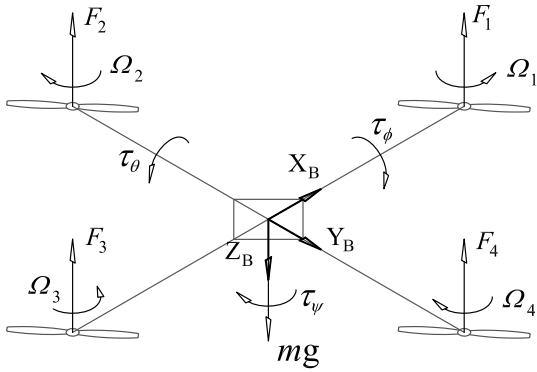
Figure 1. Quadrotor Configuration
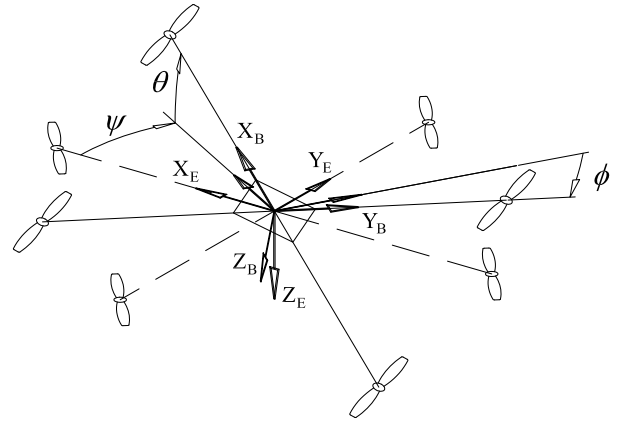
Figure 2. Euler Angles - Rotation

three basic rotation matrices, and is given as:

$$\mathfrak{R} = \begin{bmatrix} C\psi C\theta & C\psi S\theta S\phi - C\phi S\psi & C\psi C\phi S\theta + S\psi S\phi \\ C\theta S\psi & C\psi C\phi + S\psi S\theta S\phi & C\phi S\psi S\theta - C\psi S\phi \\ -S\theta & C\theta S\phi & C\theta C\phi \end{bmatrix}, \tag{1}$$

where $S(.)$ means sen(.) and $C(.)$ means cos(.), and ϕ, θ and ψ represent the roll, pitch and yaw Euler angles, respectively.

Applying Newton's equation to quadrotor leads to

$$m\ddot{\mathbf{\Gamma}}^E = \mathbf{F}^E + \mathbf{F}^E_G \tag{2}$$

where $\mathbf{\Gamma}^E = [x\ y\ z]^T$ is the cartesian coordinates of the center of gravity, $\mathbf{F}^E$, are the forces acting on the quadrotor structure (excluding the gravity force) and, $\mathbf{F}^E_G = [0\ 0\ mg]^T$, is the gravitational force vector where, m, represents the mass of the quadrotor and g, is the gravity acceleration. The expression of $\mathbf{F}^E$ is detailed in the Section 2.2.

Taking moments about the origin of the body frame, O_B, Euler's equation for the quadrotor is given by:

$$\boldsymbol{\omega}^E \times \mathbf{I}^E \boldsymbol{\omega}^E + \mathbf{I}^E \dot{\boldsymbol{\omega}}^E = \boldsymbol{\tau}^E \tag{3}$$

where $\boldsymbol{\omega}$ is the quadrotor angular velocity, $\mathbf{I}$ is the inertia matrix and $\boldsymbol{\tau}$ are the torques acting on the quadrotor structure around the body axes. Now, considering that $\mathbf{I}^E = \mathfrak{R}\mathbf{I}^B\mathfrak{R}^T$, $\boldsymbol{\tau}^E = \mathfrak{R}\boldsymbol{\tau}^B$ and $\boldsymbol{\omega}^E = \mathfrak{R}\boldsymbol{\omega}^B$, the Eq. (3) can be written in frame {**B**} as:

$$\boldsymbol{\omega}^B \times \mathbf{I}^B \boldsymbol{\omega}^B + \mathbf{I}^B \dot{\boldsymbol{\omega}}^B = \boldsymbol{\tau}^B \tag{4}$$

Equ. (4) can be rewritten as:

$$\dot{\boldsymbol{\omega}}^B = \left(\mathbf{I}^B\right)^{-1}\left(\boldsymbol{\tau}^B - \widetilde{\boldsymbol{\omega}}^B \mathbf{I}^B \boldsymbol{\omega}^B\right) \tag{5}$$

where $\widetilde{\boldsymbol{\omega}}^B$ is a skew symmetric matrix represented as:

$$\widetilde{\boldsymbol{\omega}}^B = \begin{bmatrix} 0 & -r & q \\ r & 0 & -p \\ -q & p & 0 \end{bmatrix}, \tag{6}$$

and where $\boldsymbol{\omega}^B = [p\ q\ r]^T$. Euler time derivatives are related to body angular rates as:

$$\dot{\mathbf{\Theta}} = \mathbf{T}_\theta \boldsymbol{\omega}^B \tag{7}$$

where the tranfer function, $\mathbf{T}_\theta$, is given as:

$$\mathbf{T}_\theta = \begin{bmatrix} 1 & S\phi T\theta & C\phi T\theta \\ 0 & C\phi & -S\phi \\ 0 & S\phi/C\theta & C\phi/C\theta \end{bmatrix}; \tag{8}$$

and where $\dot{\mathbf{\Theta}} = [\dot{\phi}\ \dot{\theta}\ \dot{\psi}]^T$. By diferentiating Eq. (7) with respect to time, one gets:

$$\ddot{\mathbf{\Theta}} = \dot{\mathbf{T}}_\theta \boldsymbol{\omega}^B + \mathbf{T}_\theta \dot{\boldsymbol{\omega}}^B \tag{9}$$

Substituting Eq.(5) in Eq.(9) and simplifying, one gets:

$$\ddot{\boldsymbol{\Theta}} = \dot{\mathbf{T}}_\theta \mathbf{T}_\omega \dot{\boldsymbol{\Theta}} + \mathbf{T}_\theta \left(\mathbf{I}^B\right)^{-1} \left(\boldsymbol{\tau}^B - \widetilde{\boldsymbol{\omega}}^B \mathbf{I}^B \boldsymbol{\omega}^B\right) \tag{10}$$

where $\mathbf{T}_\omega = \mathbf{T}_\theta^{-1}$. Next, by taking the product of both sides of Eq. (10) by $\mathbf{I}^B \mathbf{T}_\omega$ and simplifying, one gets:

$$\mathbf{M}(\boldsymbol{\Theta})\ddot{\boldsymbol{\Theta}} + \mathbf{C}(\boldsymbol{\Theta}, \dot{\boldsymbol{\Theta}})\dot{\boldsymbol{\Theta}} = \boldsymbol{\tau}^B \tag{11}$$

where:

$$\mathbf{M}(\boldsymbol{\Theta}) = \mathbf{I}^B \mathbf{T}_\omega; \qquad \mathbf{C}(\boldsymbol{\Theta}, \dot{\boldsymbol{\Theta}}) = -\left(\mathbf{I}^B \dot{\mathbf{T}}_\omega + \widetilde{\boldsymbol{\Lambda}} \mathbf{I}^B \mathbf{T}_\omega\right) \tag{12}$$

and where $\widetilde{\boldsymbol{\Lambda}}$ is a ske-symmetric matrix associated to the vector $\boldsymbol{\Lambda} = \mathbf{T}_\omega \dot{\boldsymbol{\Theta}}$. The expression of $\boldsymbol{\tau}^B$ is detailed in the Section 2.2.

2.2 Aerodynamics forces and torques

As pointed out above, the force produced for each motor is proprotional to the square of its angular speed rotation Ω_i, i.e, $F_i = b\Omega_i^2$, where the parameter b depends of the propeller geometry, air density, aerodynamic lift coefficient and others factors. Thus, the lift force vector is given as:

$$\mathbf{F}_T^B = \begin{bmatrix} 0 & 0 & -(F_1 + F_2 + F_3 + F_4) \end{bmatrix}^{\mathrm{T}} = \begin{bmatrix} 0 & 0 & -b\left(\Omega_1^2 + \Omega_2^2 + \Omega_3^2 + \Omega_4^2\right) \end{bmatrix}^{\mathrm{T}} \tag{13}$$

Drag forces due to translational movement of quadrotor and wind disturbance are modeled as:

$$\mathbf{F}_D^E = -\mathbf{K}_D \dot{\boldsymbol{\Gamma}}^E; \qquad \mathbf{F}_W^E = \mathbf{K}_D \mathbf{W}^E \tag{14}$$

where $\mathbf{K}_D = \mathrm{diag}(K_{dx}, K_{dy}, K_{dz})$ and $\mathbf{W}^E$ is the wind velocity vector. Therefore, the translational dynamic equation can written as:

$$m\ddot{\boldsymbol{\Gamma}}^E = \Re\mathbf{F}_T^B + \mathbf{F}_G^E + \mathbf{K}_D\left(\mathbf{W}^E - \dot{\boldsymbol{\Gamma}}^E\right) \tag{15}$$

By changing the rotor speeds moments can be generated on the airframe. So, Airframe torques are given as:

$$\boldsymbol{\tau}_P^B = \begin{bmatrix} d(F_2 - F_4) \\ d(F_1 - F_3) \\ \tau_1 + \tau_3 - \tau_2 - \tau_4 \end{bmatrix} = \begin{bmatrix} db(\Omega_2^2 - \Omega_4^2) \\ db(\Omega_1^2 - \Omega_3^2) \\ k(\Omega_1^2 + \Omega_3^2 - \Omega_2^2 - \Omega_4^2) \end{bmatrix} = \begin{bmatrix} \tau_\phi \\ \tau_\theta \\ \tau_\psi \end{bmatrix} \tag{16}$$

where d is the distance from the origin of the body frame, O_B, to the rotation axe of propeller and τ_i is the quadrotor moment generated by the ith rotor about $\mathbf{Z}_B$ axis and it is proprotional to the square of its angular speed rotation Ω_i, i.e, $\tau_i = k\Omega_i^2$, where k depends of the propeller geometry, air density, aerodynamic drag coefficient and others factors.

Gyroscopic torques, caused by combination of rotations of four propellers are derivaded as:

$$\boldsymbol{\tau}_{Gy}^B = J_p \sum_{i=1}^4 \boldsymbol{\omega}^B \times \begin{bmatrix} 0 & 0 & 1 \end{bmatrix}^{\mathrm{T}} (-1)^{i+1}\Omega_i = J_P \Omega \mathbf{T}_\omega^{-1}[\dot{\theta} \quad -\dot{\phi} \quad 0]^{\mathrm{T}} \tag{17}$$

where $\Omega = \Omega_1 - \Omega_2 + \Omega_3 - \Omega_4$ and J_p is the moment of inertia of the rotor.

Drag torques due to rotational movement of quadrotor and wind disturbance torques are modeled as:

$$\boldsymbol{\tau}_D^B = \mathbf{K}_m \dot{\boldsymbol{\theta}}; \qquad \boldsymbol{\tau}_W^B = [\tau_{wx} \quad \tau_{wy} \quad \tau_{wz}]^{\mathrm{T}} \tag{18}$$

where $\mathbf{K}_m = \mathrm{diag}(K_{mx}, K_{my}, K_{mz})$. Therefore, the rotational dynamic equation can written as:

$$\mathbf{M}(\boldsymbol{\Theta})\ddot{\boldsymbol{\Theta}} + \mathbf{C}(\boldsymbol{\Theta}, \dot{\boldsymbol{\Theta}})\dot{\boldsymbol{\Theta}} = \boldsymbol{\tau}_P^B + \boldsymbol{\tau}_{Gy}^B + \boldsymbol{\tau}_D^B + \boldsymbol{\tau}_W^B \tag{19}$$

Equations (15) and (19) determine the full dynamic model of the quadrotor.

3. QUADROTOR CONTROLLER DESIGN

As can be observed from Equations (15) and (19), the quadrotor is an underactuated system, i.e, 6 DOF with only 4 inputs (propeller angular velocities). In other words, attitude and vertical motion do not depend on horizontal motion. On the other hand, the horizontal motion depend on the attitude. That property usually is used to divide the control system in an inner loop control of attitude and vertical motion and an outer loop translational control. Thus, the desired trajectory is the horizontal position and the outer loop controller generates the attitude references.

In this paper, as an initial work, will be considered only the control of attitude, that is, the quadrotor is mounted on a stand in order to give the possibility to create attitude control without the risk of crashing the machine. In Future work, the quadrotor can be dismounted from the stand and placed on the ground and the translational controllers can be implemented.

3.1 Imperfect compensantion of the inverse dynamcis control

Inverse dynamics control is an approach to nonlinear control design of which the central idea is to construct an inner loop control which, in the ideal case, exactly linearizes the nonlinear system and an outer loop control to drive tracking errors to zero. However, from an implementation viewpoint, compensantion may be impefect, both for model uncertainties and for external disturbances, and for the approximation made of the dynamic model.

Equation (19) can be written as

$$\mathbf{M}(\boldsymbol{\Theta})\ddot{\boldsymbol{\Theta}} + \mathbf{N}(\boldsymbol{\Theta}, \dot{\boldsymbol{\Theta}}) = \mathbf{u}_T + \boldsymbol{\tau}_{dist}^B, \tag{20}$$

where

$$\boldsymbol{\tau}_{dist}^B = \boldsymbol{\tau}_{Gy}^B + \boldsymbol{\tau}_D^B + \boldsymbol{\tau}_W^B \quad ; \quad \mathbf{N}(\boldsymbol{\Theta}, \dot{\boldsymbol{\Theta}}) = \mathbf{C}(\boldsymbol{\Theta}, \dot{\boldsymbol{\Theta}})\dot{\boldsymbol{\Theta}},$$

and where $\mathbf{u}_T = \boldsymbol{\tau}_P^B$ which is proportional to vector voltage or current (not considering the motor electrical dynamics) driving the propeller.

The robust law control can be expressed by (Figure 3)

$$\mathbf{u}_T = \widehat{\mathbf{M}}(\boldsymbol{\Theta})\mathbf{v} + \widehat{\mathbf{N}}(\boldsymbol{\Theta}, \dot{\boldsymbol{\Theta}}); \tag{21}$$

where $\widehat{\mathbf{M}}, \widehat{\mathbf{N}}$ represent simplified versions of $\mathbf{M}, \mathbf{N}$, and

$$\mathbf{v} = \ddot{\boldsymbol{\Theta}}_d + \mathbf{K}_d\dot{\mathbf{e}} + \mathbf{K}_p\mathbf{e} + \mathbf{u}; \tag{22}$$

and

$$\begin{aligned} \mathbf{K}_p &= \text{diag}\left\{\omega_1^2, ..., \omega_6^2\right\} \\ \mathbf{K}_d &= \text{diag}\left\{2\varsigma_1\omega_1, ..., 2\varsigma_6\omega_6\right\} \end{aligned} \tag{23}$$

and where the tracking error is defined as

$$\mathbf{e} = \boldsymbol{\Theta}_d - \boldsymbol{\Theta}; \tag{24}$$

where $\boldsymbol{\Theta}_d$ is the desired cartesian space coordinates.
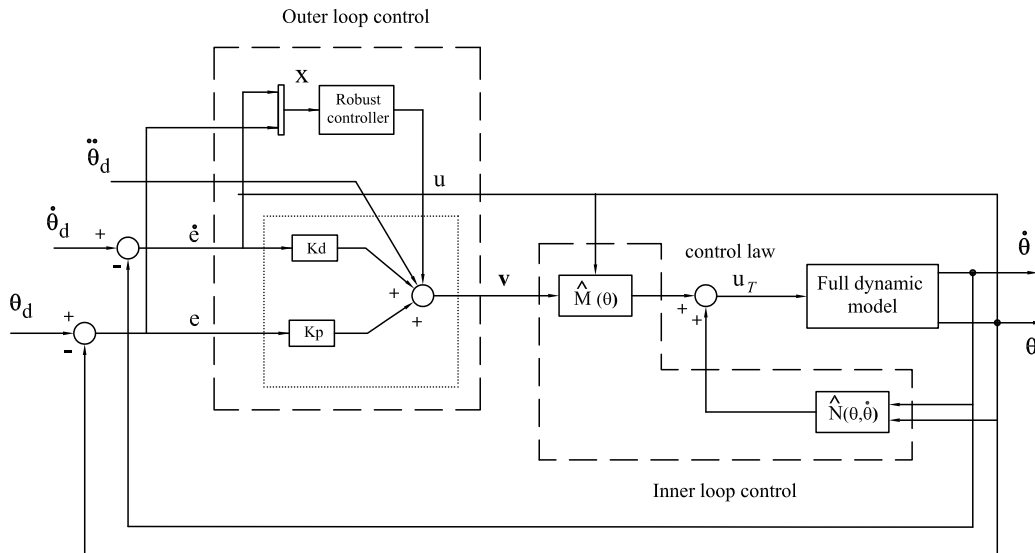
Figure 3. Inverse Dynamic Control, Imperfect Compensantion

The term $\mathbf{u}$ in Eq. (22) is included to overcome imperfect compensation effects. Now, substituting Eq. (21) into Eq. (20) and simplifying it, one gets

$$\ddot{\mathbf{e}} + \mathbf{K}_d\dot{\mathbf{e}} + \mathbf{K}_p\mathbf{e} = \mathbf{w} - \mathbf{u}; \tag{25}$$

where

$$\begin{aligned} \mathbf{w} &= (\mathbf{I} - \mathbf{M}^{-1}\widehat{\mathbf{M}})\mathbf{v} - \mathbf{M}^{-1}\Delta\mathbf{N} - \mathbf{M}^{-1}\boldsymbol{\tau}_{dist}^B; \\ \Delta\mathbf{N} &= \mathbf{N} - \widehat{\mathbf{N}} \end{aligned} \tag{26}$$

In state space representation the system described by Eq. (25) becomes

$$\dot{\mathbf{x}} = \mathbf{A}\mathbf{x} + \mathbf{B}(\mathbf{w} - \mathbf{u})$$
$$\mathbf{y} = \mathbf{x} \tag{27}$$

where

$$\mathbf{A} = (\mathbf{H} - \mathbf{B}\mathbf{K}) \ , \quad \mathbf{K} = \begin{bmatrix} \mathbf{K}_\mathrm{p} & \mathbf{K}_\mathrm{d} \end{bmatrix} \tag{28}$$

and

$$\mathbf{H} = \begin{bmatrix} \mathbf{0} & \mathbf{I} \\ \mathbf{0} & \mathbf{0} \end{bmatrix} \ \mathbf{B} = \begin{bmatrix} \mathbf{0} \\ \mathbf{I} \end{bmatrix} \ \mathbf{x} = \begin{bmatrix} \mathbf{e} \\ \dot{\mathbf{e}} \end{bmatrix} \tag{29}$$

In this context, the term $\mathbf{u}$ must be designed to stabilize the nonlinear time-varying error system defined by Eq. (27) in the presence of the incertainty $\mathbf{w}$. In the next section, the strategy will be designed in order to find this term.

3.2 Robust outer loop design by Lyapunov's Second Method

To determine $\mathbf{u}$ one can consider the following positive definite quadratic form as Lyapunov function candidate:

$$\mathbf{V} = \mathbf{x}^\mathrm{T}\mathbf{P}\mathbf{x} > 0 \qquad \forall \mathbf{x} \neq 0 \tag{30}$$

The time derivative of $\mathbf{V}$ is:

$$\frac{d\mathbf{V}}{dt} = -\mathbf{x}^\mathrm{T}\mathbf{T}\mathbf{x} + 2\mathbf{x}^\mathrm{T}\mathbf{P}\mathbf{B}(\mathbf{w} - \mathbf{u}), \tag{31}$$

where

$$\mathbf{A}^\mathrm{T}\mathbf{P} + \mathbf{P}\mathbf{A} = -\mathbf{T}, \tag{32}$$

for any symmetric positive definite matrix $\mathbf{T}$ and considering that $\mathbf{A}$ has eigenvalues with all real parts negative. If $d\mathbf{V}/dt$ is negative then the system represented by the Eq. (27) converge to zero. Thus, the term $\mathbf{u}$ is chosen to render the second term in Eq. (31) less than or equal to zero, and it is given as:

$$\mathbf{u} = \frac{\rho}{\|\mathbf{z}\|}\mathbf{z} \quad \rho > 0 \quad ; \tag{33}$$

where

$$\mathbf{z} = \mathbf{B}^\mathrm{T}\mathbf{P}\mathbf{x}; \tag{34}$$

and where

$$\rho \geq \frac{1}{1-\lambda}\left(\lambda Q_M + \lambda \|\mathbf{K}\| \|\mathbf{x}\| + B_M\Phi - B_M\Psi\right) \tag{35}$$

The scalar values Q_M, λ, B_M, Φ and Ψ represent a worst case bound on the incertanty $\mathbf{w}$ in Eq. (26) and they are given as

$$\sup_{t \geq 0} \left\|\ddot{\mathbf{\Theta}}_\mathrm{d}\right\| < Q_M < \infty \quad \forall \ddot{\mathbf{\Theta}}_\mathrm{d}$$

$$\left\|\mathbf{I} - \mathbf{M}^{-1}\widehat{\mathbf{M}}\right\| \leq \lambda \leq 1 \quad \forall \mathbf{\Theta}$$

$$\|\Delta\mathbf{N}\| \leq \Phi \leq \infty \quad \forall \mathbf{\Theta}, \dot{\mathbf{\Theta}} \tag{36}$$

$$\left\|\mathbf{M}^{-1}\right\| \leq B_M \quad \forall \mathbf{\Theta}$$

$$\left\|\tau_{dist}^B\right\| \leq \Psi \leq \infty$$

3.2.1 Sliding surfaces

The robust control law in Eq. (33) guarantees existence of individual sliding modes in the sliding subspace $\mathbf{z} = 0$. A characterization of an error trajectory is given by considering the sliding subspace as:

$$\mathbf{z} = \mathbf{B}^{\mathrm{T}}\mathbf{Px} = \begin{bmatrix} ae_1 & + & b\dot{e}_1 \\ \vdots & \vdots & \vdots \\ ae_6 & + & b\dot{e}_6 \end{bmatrix} = \mathbf{0}; \tag{37}$$

so, for all $e_i(0)$ and $\dot{e}_i(0) \notin$ null space of the sliding surfaces $ae_i + b\dot{e}_i = 0$, the error trajectory is attracted on the sliding surfaces and tends towards the origin.

The control law defined in Eq. (33) presents a phenomen kwown as chattering, which is often undesirable since the high frequency oscillations in the control can excite unmodeled dynamic effects. Elimination of chattering can be achieved by introducing a boudary layer that contains the sliding surface. The introduction of the boundary layer is equivalent to the replacement of the control law in Eq. (33) by a saturation function as

$$\mathbf{u} = \begin{cases} \dfrac{\rho}{\|\mathbf{z}\|}\mathbf{z} & \forall\, \|\mathbf{z}\| \geq \epsilon \\[2ex] \dfrac{\rho}{\epsilon}\mathbf{z} & \forall\, \|\mathbf{z}\| < \epsilon \end{cases} \tag{38}$$

Although the control law in Eq. (38) does not guarantee error convergence to zero, it ensures bounded-norm error given by ϵ. The idea of the boundary layer is illustrated on Figure 4, where the layer thickness, ϵ_t, the slope of the sliding line, λ_s, and the layer width, ϵ_w, are given as:

$$\epsilon_t = \epsilon/b; \quad \lambda_s = -a/b; \quad \epsilon_w = \epsilon_t/\lambda_s; \tag{39}$$

where a and b are defined in Eq. (37). The slope of the sliding line, λ_s, depends principally on matrix $\mathbf{P}$ in Eq. (32).
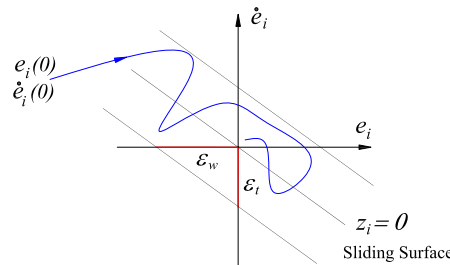
Figure 4. Error Trajectory with Robust Control and Chattering Elimination

3.3 Simplification of the matrices of the control law

The coefficient matrices of Eq.(21) can be approximated to constant ones. Based on these constant matrices, calculation of the approximated inverse dynamics becomes much simpler reducing computation time significantly. In this context, matrices $\widehat{\mathbf{M}}(\boldsymbol{\Theta})$ and $\widehat{\mathbf{N}}(\boldsymbol{\Theta}, \dot{\boldsymbol{\Theta}})$ considered in the law control in Eq.(21), are defined as:

$$\begin{aligned} \widehat{\mathbf{M}}(\boldsymbol{\Theta}) &= \mathbf{I}^{\mathrm{B}} \\ \widehat{\mathbf{N}}(\boldsymbol{\Theta}, \dot{\boldsymbol{\Theta}}) &= \mathbf{0} \end{aligned} \tag{40}$$

4. NUMERICAL SIMULATION

The performance of the proposed controllers is verified by numerical simulations and results are presented in Fig 5. Geometric and inertia properties are shown in Table 1 and were got from Goel *et al.* (2009). Desired trajectory in pitch direction (θ) were generated from 3rd order polynomial while desired trajectory in roll (ϕ) and yaw (ψ) directions are equal to zero. The Runge-Kutta fourth-order numerical integration method is used to solve the ordinary differential equation of the dynamic model. Computer codes are written in MATLAB.

The sliding surface parameters a, b and ϵ, in Eqs.(37) and (38) was choosen as 0.0102, 0.0607 and 0.002, respectively. Too small values of ϵ can lead to instability problems. The simulation sample time was choosen to be 0.001. For a relatively low sampling frequency, the limited switching frequency in Eq. (33) can lead to undesirable effects in the input signal or even instability of the closed-loop system (Monsees, 2002).

Pitch attitude response and angular velocities of the propellers are shown in Fig. 6. From Figs. 5 and 6 can be observed chattering phenomen was eliminated and smoothed angular velocities were generated. The quadrotor realized the pitch trajectory tracking with very good robustness to the unmodeled dynamics and external disturbances, and the parasitic pitch and yaw motion are equal (or almost) to zero.

Table 1. Quadrotor Parameters

d	0.38	m	m	4.493	Kg	
k	3.24×10^{-6}	N.m.s²/rad	J_p	1.46×10^{-3}	Kg.m² /rad	
b	8.8×10^{-5}	N.s²/rad	I_x, I_y	0.177	Kg.m²	
K_{mx}, K_{my}, K_{mz}	0.35	N.m.s/rad	I_z	0.334	Kg.m²	

(a) Pitch attitude response

(b) Yaw and roll attitude reponse
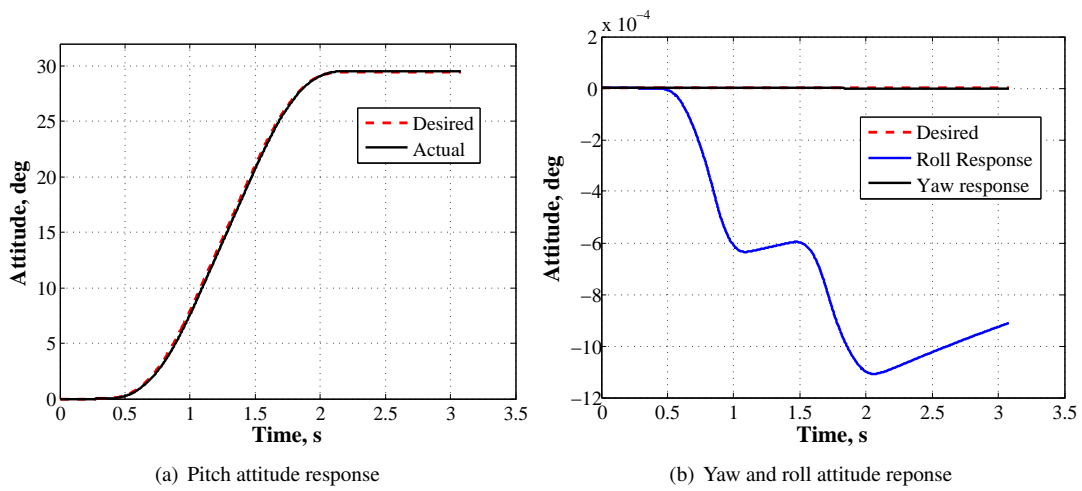
Figure 5. Quadrotor response
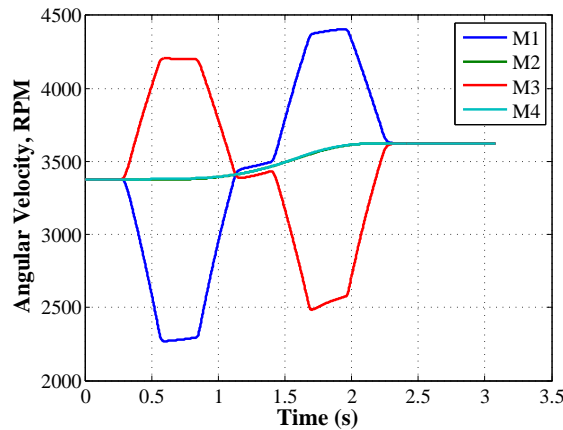
Figure 6. Propeller angular velocities

5. CONCLUSIONS

In this paper, a control approach for the attitude control of a quadrotor was presented. A full dynamic model was develeped. The controller was implemented in the outer loop of the inverse dynamic control scheme in order to counteract imperfect compensation and external disturbances. The approachs was designed via Lyapunov stability theory. Chattering reduction was achieved by saturarion control. The controller presented robustness to bounded modelling error and chattering phenomen was eliminated.

6. REFERENCES

Bauer, P., Ritzinger, G., Soumelidis, A. and Bokor, J., 2008. "LQ servo control design with kalman filter for a quadrotor UAV". *Transportation Engineering*, Vol. 36, No. 1-2, pp. 9–14.

Becerra-Vargas, M., Belo, E.M. and Grant, P.R., 2009. "Robust control of a flight simulator motion base". In *AIAA Modeling and Simulation Technologies Conference*. AIAA, Chicago, IL, pp. 1–13.

Benallegue, A., Morhtari, A. and Fridman, L., 2008. "High-order sliding-mode observer for a quadrotor UAV". *International Journal of Robust and Nonlinear Control*, Vol. 18, No. 4, pp. 10–12.

Bouabdallah, S., Noth, A. and Siegwart, R., 2004. "PID vs LQ control techniques applied to an indoor micro quadrotor". In *Proceedings of the 2004 IEEE/RSJ International Conference on Intelligent Robots and Systems*. Vol. 3.

Bouabdallah, S. and Siegwart, R., 2007. "Full control of a quadrotor". In *Proceedings of the 2007 IEEE/RSJ International Conference on Intelligent Robots and Systems*.

Goel, R., Shah, S.M., Gupta, N.K. and Ananthkrishnan, N., 2009. "Modeling, simulation and flight testing of an autonomous quadrotor". In *IISc Centenary International Conference and Exhibition on Aerospace Engineering*.

Guisser, M. and Medromi, H., 2009. "A high gain observer and sliding mode controller for an autonomous quadrotor helicopter". *International Journal of Intelligent Control and Systems*, Vol. 14, No. 3, pp. 204–212.

Lee, D., Kim, H.J. and Sastry, S., 2009. "Feedback linearization vs. adaptive sliding mode control for a quadrotor helicopter". *International Journal of Control, Automation, and Systems*, Vol. 7, No. 3, pp. 419–428.

Mian, A.A. and Daobo, W., 2008. "Modeling and backstepping-based nonlinear control strategy for a 6 DOF quadrotor helicopter". *Chinese Journal of Aeronautics*, Vol. 21, No. 3, pp. 261–268.

Mokhtari, A., Benallegue, A. and Daachi, B., 2007. "Robust inner outer controller and sliding mode observer for a quadrotor UAV". *International Journal of Automation, Robotics and Autonomous Systems - ARAS*, Vol. 6, No. 1, pp. 17–26.

Monsees, G., 2002. *Discrete-Time Sliding Mode Control*. Ph.D. thesis, Delft University of Technology, Netherlands.

Xu, R. and Ozguner, U., 2006. "Sliding mode control of a quadrotor helicopter". In *Proceedings of the 45th IEEE Conference on Desicion & Control*.

7. Responsibility notice

The author(s) is (are) the only responsible for the printed material included in this paper